Design and Commercial Operation of a Discretely Heat Integrated Distillation Column

Toshihiro Wakabayashi[a,*], Alessandro Ferrari[b], Shinji Hasebe[c]

[a]Toyo Engineering Corporation, 2-8-1 Akanehama, Narashino-shi, Chiba 275-0024, Japan
[b]Koch-Glitsch Italia Srl-Unipersonale, Via Torri Bianche, 3/A 20871 Vimercate (MB), Italy
[c]Kyoyo University, Katsura Campus, Kyoto 615-8510, Japan
toshihiro.wakabayashi@toyo-eng.com

In the conventional heat integrated distillation column (HIDiC), the optimal heat exchange cannot be achieved because the heat exchange between the rectifying section and the stripping section is executed through the wall at the physically same elevation. To be released from this constraint, authors have proposed a new process structure in which the heat exchange is executed between several pairs of stages in the rectifying and stripping sections, and such HIDiC is hereafter called the discrete HIDiC (D-HIDiC). Authors have also developed a new graphical design procedure for D-HIDiC, in which a plausible design is interactively derived using the extended Ponchon-Savarit *H-xy* diagram. The proposed procedure was applied to a design problem of commercially operated column and subsequently D-HIDiC was applied at Maruzen Petrochemical Co. Ltd., Japan. Through the stable operation since August in 2016, it was verified that more than 55% energy conservation to the conventional distillation column could be achieved.

In this research, the design and operating conditions of the commercially operating D-HIDiC are explained. Though the pairing of heat exchange stages cannot be changed in the commercial operation, the column has a function of adjusting the heat exchange rate at each side heat exchanger. By using this function, the heat allocation to side heat exchangers is modified so that the heat allocation is close to the optimal condition. The effect of proper allocation of heat to the side heat exchangers on the energy-saving performance is discussed using the actual operating data. It was demonstrated that appropriate side heat exchanger allocation having similar composition-enthalpy change as the reversible distillation can achieve higher energy conservation.

1. Introduction

Since the concept of the heat integrated distillation column (HIDiC) was proposed by Mah et al. (1977), many researchers have attempted to verify its energy-saving performance. For instance, Horiuchi et al. (2008) constructed a pilot plant consisting of double pipe structure. Bruinsma et al. (2010) made experiments with plate fin type structure in labo-scale apparatus. The structures of HIDiC proposed so far assume that the rectifying and the stripping sections are installed in parallel, and the internal heat exchange is executed through the wall between the rectifying and stripping sections. Such HIDiC is hereafter called the conventional HIDiC. Although many types of research have been made on the conventional HIDiC, there has been no commercial application. This is because it has inherent drawbacks for realizing its concept such as the difficulty of the maintenance. One of the serious drawbacks is that the internal heat exchanges cannot be optimized since the heat is transferred through the wall at the physically same elevation. Authors showed that better energy conservation could be derived by executing the heat exchange at several pairs of stages in the rectifying and stripping sections (Wakabayashi and Hasebe, 2011). Moreover, authors developed a new design methodology to derive the optimal heat exchanger arrangement. In the proposed methodology, a plausible heat exchange manner is interactively obtained by the graphical approach using the extended Ponchon-Savarit *H-xy* diagram (Wakabayashi and Hasebe, 2013). Furthermore, authors extended the proposed methodology to multi-component system and proposed a new HIDiC structure to realize outcomes through the developed design methodology (Wakabayashi and Hasebe, 2015).

The D-HIDiC having the proposed structure has been applied to a commercially operated chemical plant to

replace the existing conventional distillation column in Maruzen Petrochemical Co. Ltd., Japan. The D-HIDiC is being operated stably since August in 2016. Though the assignment of heat to each heat exchange at the beginning of the plant operation was not exactly similar to that derived by the proposed design procedure, the energy conservation of more than 55% to the conventional distillation column was achieved. In this paper, the effect to the energy conservation of the re-arrangement of heat allocation is disclosed, and the effect of proper allocation of heat to the side heat exchangers is discussed.

2. Design Methodology

The process flow scheme of the proposed D-HIDiC is shown in Figure 1. By compressing the vapor from the stripping section to the rectifying section, the vapor in the rectifying section can be used to vaporize the liquid in the stripping section. The heat exchanger used for this purpose is hereafter called the side heat exchanger (SHX). In this section, the outline of the design procedure of D-HIDiC is explained. The details have been described in Wakabayashi and Hasebe (2015). The unique feature of the proposed design method is that two dominant design variables related to the performance of the energy conservation, reboiler duty, Q_R, and compressor power, W_S, are first assumed in referring to the reboiler duty of the conventional distillation column, $Q_{R\text{-conv}}$. The operating pressure in the stripping section, P_s, and the number of SHXs are also determined in advance. Then, the arrangement of SHXs is decided by using the extended $H\text{-}xy$ diagram. The number of theoretical stages, NTS, at each section, the operating pressure in the rectifying section, P_r, and the heat transfer area for each SHX are derived as a result of the design procedure. The design steps are explained in referring to Figure 2.

Step 1: For the given feed and product conditions, $Q_{R\text{-conv}}$ and the NTS, $N_{T\text{-conv}}$, for a conventional column are calculated. The operating pressure is assumed to be the same as that in the stripping section of D-HIDiC, P_s.

Step 2: The target values of Q_R and W_S in D-HIDiC are determined in referring to $Q_{R\text{-conv}}$. The NTS in the stripping and rectifying sections of D-HIDiC are also assumed in referring to $N_{T\text{-conv}}$.

Step 3: $H\text{-}xy$ diagram shown in Figure 2 is used to derive the design variables of D-HIDiC. First, the enthalpy curves at saturated conditions and the equilibrium lines, EqLs, of the stripping section are provided ((1)EqL in Figure 2), and the reversible distillation curve, RDC, in the stripping section is drawn ((2)RDC in Figure 2).

Step 4: The curve obtained by shifting the RDC downward is hereafter called the shifted reversible distillation curve, S-RDC ((3)S-RDC in Figure 2). The NTS in the stripping section is graphically derived by using the EqLs and the S-RDC. The distance between RDC and S-RDC is adjusted so that the NTS takes the pre-specified value.

Step 5: The operating locus, OpL, is depicted to overlap S-RDC ((4)OpL in Figure 2). In the example of Figure 2, four SHXs are installed, and q_i in Figure 2 corresponds to the amount of heat transferred at the i-th SHX. B in the figure is the bottom molar flow rate.

Step 6: The NTS in the stripping section is graphically derived by using the EqLs and the OpL. If the derived number is not adequate, the OpL is adjusted by changing the composition where the heat is supplied and/or by changing the heat duty at each SHX.

Step 7: The operating pressure in the rectifying section, P_r, is calculated by Eq. (1).

$$W_S = \frac{V_{\text{in}}}{\eta} \frac{\gamma}{\gamma - 1} R T_{\text{in}} \left[\left(\frac{P_r}{P_s} \right)^{\gamma - 1/\gamma} - 1 \right] \tag{1}$$

Here, V_{in}, T_{in} and γ are the vapor molar flow rate, temperature and specific heat ratio respectively at the inlet of the compressor, which can be regarded as the vapor ascending from the top of the stripping section (See Figure 1). The details can be referred to Wakabayashi and Hasebe (2013).

Step 8: The enthalpy curves at saturated conditions and the EqLs in the rectifying section are provided ((5)EqL in Figure 2), and the RDC in the rectifying section is drawn ((6)RDC in Figure 2).

Step 9: From the overall heat balance ((7)OHBL in Figure 2), the position of the S-RDC in the rectifying section can be determined ((8) S-RDC in Figure 2). Then, the NTS is confirmed when the composition-enthalpy change is provided in accordance with the S-RDC. If the derived number is not adequate, return to Step 4 and re-allocate the overall NTS to the stripping and rectifying sections.

Step 10: The OpL is depicted to overlap the S-RDC ((9)OpL in Figure 2). As the amount of heat transferred at each SHX has been decided at Step 5-6, the size of step change of the OpL in the rectifying section must be q_i/D in the figure. Here, D is the molar flow rate of distillate. The starting point of OpL is also determined from the overall heat balance of the column ((10)OHBL in Figure 2).

Step 11: The NTS in the rectifying section is graphically derived from the EqLs and the OpL. If the derived

number is not adequate, the composition where the OpL is broken is adjusted. If it is difficult to obtain the desired NTS, return to Step 5 and readjust the OpL of the stripping section.

Step 12: By utilizing second ordinate, the bubble point temperature to the liquid composition in the stripping section is drawn on T-xy diagram ((11)BPT in Figure 2). Similarly, the dew point temperature to the vapor composition in the rectifying section is provided ((12)DPT in Figure 2).

Step 13: ΔT_1 through ΔT_4 in the figure are the temperature differences between the hot and cold streams. From these values, the heat transfer areas of SHXs are calculated. In the case where the sufficient temperature difference cannot be obtained, the profiles of the operating loci are re-examined. If such approach cannot remedy it, return to Step 2 and the target energy conservation is reconsidered.

3. Design and Operation of a Commercial Plant

Energy saving of methyl ethyl ketone (MEK) fractionator in alcohol and ketone process was explored in Maruzen Petrochemical Co. Ltd, Japan. In 2014 it was decided to replace the existing MEK fractionator with D-HIDiC system. Since its start-up in 2016, the commercial production by D-HIDiC system is being continued stably as world first commercial application of HIDiC technology. The process flow diagram of the commercial D-HIDiC system is shown in Figure 3. In this process, a part of rectifying section is moved to the low pressure column to operate at a larger relative volatility.

The feed condition of the original operating mode (operating mode 1) is shown in Table 1. Light and heavy key components are MEK and sec-butanol, respectively. The feed contains light non-key, intermediate and heavy non-key components. The specification of the distillate is MEK of 99.918 wt % and that of the bottoms is MEK of 200 wt ppm. Steam of 0.5 MPa and the electricity are available as utilities.
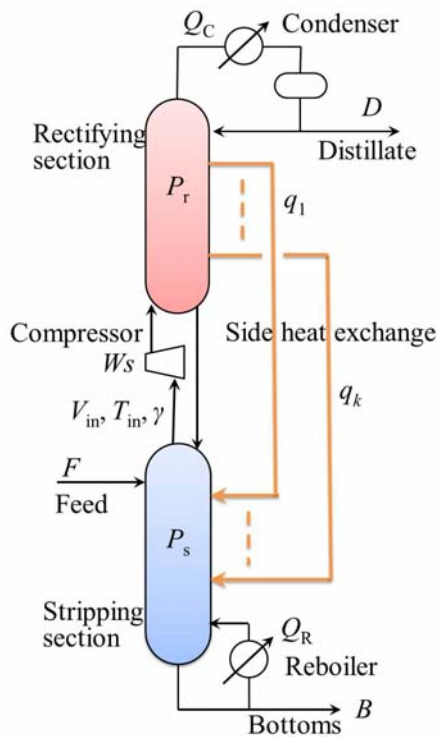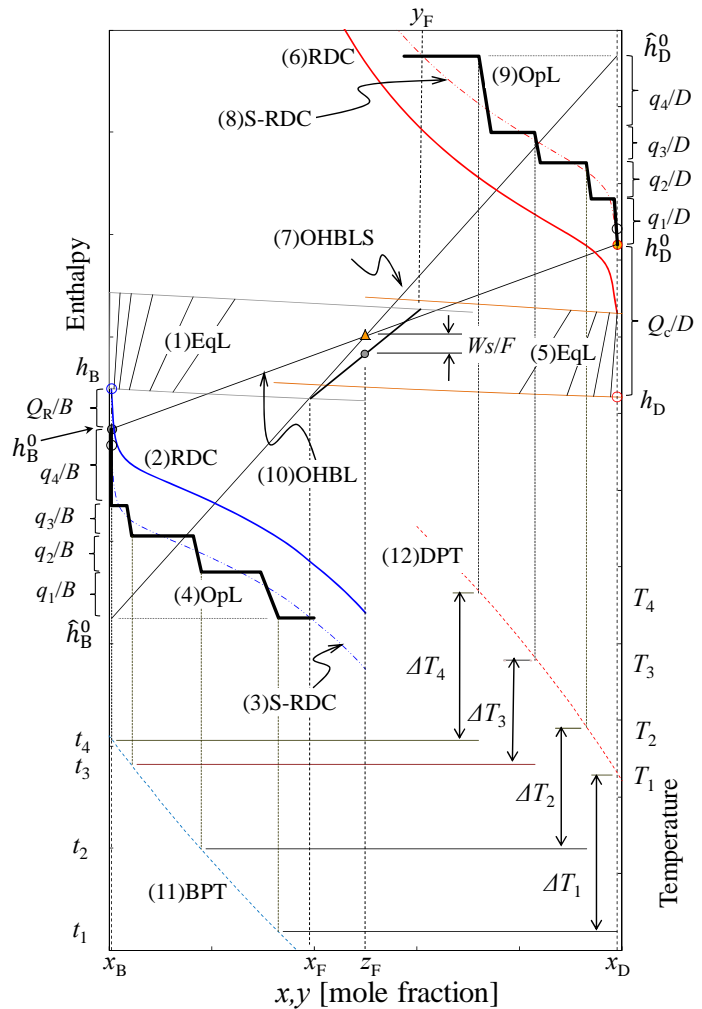

Figure 1: Brief process flow scheme

Figure 2: H-xy and T-xy diagrams that largely modified Ponchon-Savarit H-xy diagram

First, the energy consumption in the conventional distillation column, which is the datum point for the evaluation of D-HIDiC, is derived through the process simulation. The simulation model has been developed to trace the existing plant perfectly. All conditions below used in the simulation model are in line with the existing plant. The NTS corresponds to the reflux ratio of 1.11 times larger than the minimum reflux ratio, which is relatively energy-conscious design as compared with the industrial practice. The operating pressure is 102.5 kPa and 150.7 kPa at the top and bottom of the column respectively due to the pressure drop across the piping, condenser and trays. The simulation results for operating mode 1 show that $Q_{\text{R-conv}}$ is 6055 kW and the NTS of the rectifying section and that of the stripping section are 59 and 21, respectively including condenser and reboiler stages. Also, the pumps processing the condensate of overhead vapor and bottoms consume the power of 54 kW and 10 kW, respectively.

The D-HIDiC system was designed by using the methodology explained in section 2. Considering the simulation result of the conventional column, the NTS of the stripping section is set to the same value as that of the conventional column, *i.e.* 21 stages. The NTS of the high and low pressure rectifying sections are set to 8 and 34, respectively. These values are smaller than that of the conventional column, because the reflux ratio of the corresponding conventional column is smaller than that of the industrial practice. Figure 4 shows the *H-xy* and *T-xy* diagram for the condition of operating mode 1. To use the *H-xy* and *T-xy* diagram, the multi-component system must be transformed into a binary system. The details of transformation have been described in Wakabayashi and Hasebe (2015). In Figure 4, the S-RDC of the stripping section is depicted so that the stripping section has 21 stages. Then, the OpL in the stripping section is decided. In this case, the OpL is not perfectly overlapped with the S-RDC due to the design margin of fourth SHX. The actual operating conditions at operating mode 1 are illustrated in Figure 3. The reboiler duty can be decreased to 0 MW while the compressor and pumps consume the power of 917 kW and 89 kW, respectively. Here, the power includes any mechanical loss, and motor efficiency is also taken into account. Adiabatic efficiency of the compressor is derived as 70.4 %. The side heat exchange arrangement is summarized in Table 2.

4. Adjustment of the Operating Condition

In operating mode 1, the amount of heat exchanged at the fourth SHX is larger than that calculated by the design procedure. It works positive for the stripping section, but works negative for the rectifying section, because the fourth SHX is installed to the intermediate stage of the rectifying section. By taking this fact into account, the allocation of heat to the four SHXs is adjusted without changing the pairing of heat exchange stages. To synchronize the actual operating condition at that time, the feed condition is slightly changed as shown in Table 3. The specification of MEK purity in the distillate is also changed to 99.938 wt%, which is slightly higher than that at operating mode 1. The specification of MEK at the bottom stream is 200 wt ppm, which is the same as operating mode 1. This condition is hereafter called operating mode 2.

Table 1: Process conditions in operating mode 1

Flowrate	[kg/h]	15994
	[kmol/h]	219.9
Temperature	[K]	366.0
Phase	[-]	Liquid
Composition	[wt frac.]	
light non-keys		0.000158
methyl ethyl ketone		0.720506
Intermediate		0.001723
sec-butanol		0.270165
heavy non-keys		0.007448

Table 2: Side heat exch. arrangement in operating mode 1

	Paring (*)	Heat Duty	Temp. Difference
	[-]	[MW]	[K]
Side hex. #1	R1-S3	0.307	22.9
Side hex. #2	R1-S5	1.103	21.1
Side hex. #3	R1-S7	0.791	17.3
Side hex. #4	R8-S21	3.894	5.8

*: R*i*-S*j* means the heat integration between stage *i*
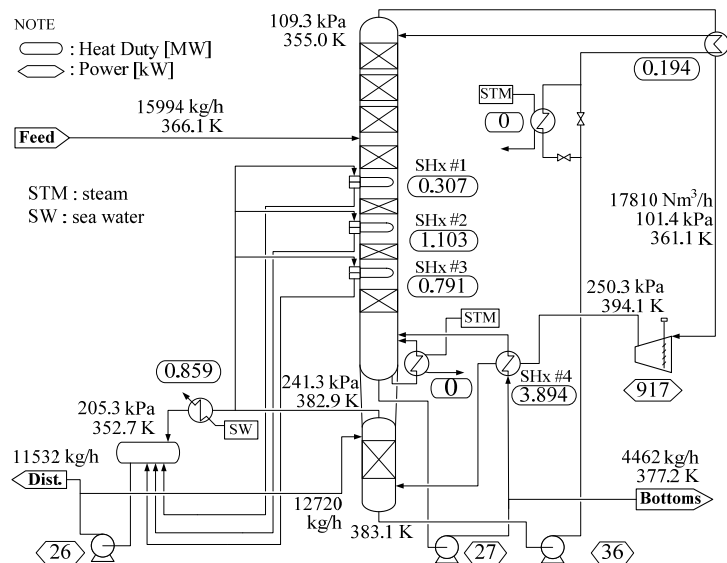and *j* in the rectifying and stripping section

Figure 3: Process flow diagram of D-HIDiC in operating mode 1

As similar to operating mode 1, the energy consumption of the conventional distillation column is derived through the process simulation with the same NTS and pressure profile as stated in section 3. The simulation result shows that $Q_{R\text{-conv}}$ is 6135 kW and the pumps processing the condensate of overhead vapor and bottoms consume 55 kW and 10 kW, respectively. The reboiler duty is larger than the case in operating mode 1 because of the severe specification of MEK in the distillate.

The result of the allocation of heat duties to SHXs is shown in Table 4 and the subsequent OpL is depicted in Figure 4 together with the OpL in operating mode 1. Though the developed $H\text{-}xy$ and $T\text{-}xy$ diagram for operating mode 2 is not completely identical to that for operating mode 1, the difference is not significant. Thus, to compare the operating loci of two operating modes in the stripping section, two operating loci are provided in the same figure. Other operating conditions are embedded in Figure 5.

In operating mode 2, the reboiler consumes the heat of 0 MW while the compressor and pumps consume the power of 915 kW and 86 kW. Adiabatic efficiency of the compressor is 62.3 %, which is significantly deteriorated to that in operating mode 1. This is because the operating point in this mode becomes far from the optimum point of the compressor. Again, this is because the compressor's impeller is unintentionally manufactured such that the optimal design point is higher than the true design point in terms of the head.

5. Evaluation of Operation in Commercial Plant

The evaluation of the energy conservation is made by comparing total energy consumption between the conventional distillation column and the D-HIDiC system. In calculating total energy consumption, the power is converted into the primary energy with the efficiency of 36.6 %. In operating mode 1, overall energy consumptions in the conventional distillation column and the D-HIDiC are 6230 kW and 2749 kW, respectively. Accordingly, the subsequent energy saving is 55.9%. Similarly, in operating mode 2, the overall energy consumption in the conventional distillation column and the D-HIDiC are 6313 kW and 2735 kW, respectively. Subsequent energy saving is 56.7 %. The apparent improvement by fine-tuning of side heat exchange arrangement is just 0.8 point; however, more improvement is expected if the compressor would work at the same adiabatic efficiency as operating mode 1. If the compressor works at the same adiabatic efficiency of 70.4 % as operating mode 1, the power consumption by compressor would be 817 kW, which results in the energy conservation of the D-HIDiC of 60.9% to the conventional distillation.

Table 3: Process conditions in operating mode 2

Flowrate	[kg/h]	15933
	[kmol/h]	218.9
Temperature	[K]	366.6
Phase	[-]	Liquid
Composition	[wt frac.]	
light non-keys		0.000085
methyl ethyl ketone		0.711498
Intermediate		0.001208
sec-butanol		0.278839
heavy non-keys		0.008297

Table 4: Side heat exch. arrangement in operating mode 2

	Paring (*)	Heat duty	Temp. Difference
	[-]	[MW]	[K]
Side hex. #1	R1-S3	1.023	20.0
Side hex. #2	R1-S5	0.953	18.7
Side hex. #3	R1-S7	0.566	13.9
Side hex. #4	R8-S21	3.511	4.4

*: Ri-Sj means the heat integration between stage i and j in the rectifying and stripping section
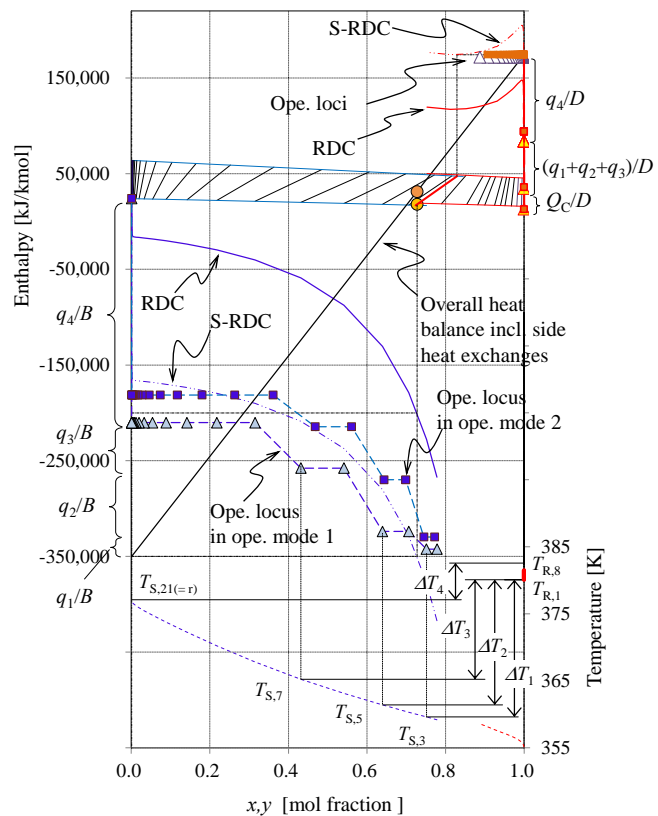

Figure 4: $H\text{-}xy$ and $T\text{-}xy$ diagrams in operating mode 1 and operation loci in two operating modes

Figure 5: Process flow diagram of D-HIDiC in operating mode 2

These operations suggest that the appropriate arrangement of heat duties to SHXs gives better energy conservation. Conversely, it is also outstanding that the D-HIDiC can derive still good level of energy conservation even with non-tuned side heat exchange arrangement. In the commercial production plant, the heat duty at each SHX may be changed due to several reasons such as the change in feed compositions, the fouling of SHXs, etc., which cannot be avoided in real operation. The robustness of the D-HIDiC in terms of heat duty allocation to the SHXs is a great benefit for industrial applications.

The high investment cost of compressor is always the problem when introducing it to the distillation processes. To evaluate the economics, the total investment cost of the proposed process and that of the conventional distillation column were calculated and the pay-out period was derived. The precise calculation result has been shown that the pay-out time is less than three years, and it is acceptable for industrial application. The details of economic evaluation are shown in Wakabayashi and Hasebe (2015).

6. Conclusions

The discretely heat integrated distillation column was applied to the commercially operated column in Maruzen Petrochemical Co. Ltd., Japan. The plant is being operated stably in achieving more than 55 % energy-saving to the conventional distillation column since 2016. Two operating modes with different side heat duty allocation were applied through commercial operation. It was demonstrated that appropriate side heat exchanger allocation having similar composition-enthalpy change as the reversible distillation can achieve higher energy conservation. It was also confirmed that the proposed discrete HIDiC showed good performance even when the heat duty allocation to the side heat exchangers fluctuates from the optimal allocation as far as heat exchangers are provided at appropriate stages. These characteristics give great flexibility in actual plant operation.

References

Bruinsma O.S.L., Tromp S.A., Strijker M., Malhotra A., Saric M., Cot J., Olujic Z., 2010, Heat Integrated Distillation using a Plate-fin Heat Exchanger, CHISA, Prague.

Horiuchi K., Nakaiwa M., Iwakabe K., Matsuda K., Toda M., 2008, Intensification of the Process Flow in the Pilot Plant of Internally Heat-Integrated Distillation Column(HIDiC), Kagaku Kogaku Ronbunshu, 34, 70–75.

Mah R.S.H., Nicholas Jr. J.J., Wodnik R.B., 1977, Distillation with Secondary Reflux and Vaporization: A Comparative Evaluation, AIChE Journal, 23, 651–658.

Wakabayashi T., Hasebe S., 2011, Effect of Internal Heat Exchange Rate Distribution on Energy Saving in Heat Integrated Distillation Column (HIDiC), Kagaku Kogaku Ronbunshu, 37, 499–505.

Wakabayashi T., Hasebe S., 2013, Design of Heat Integrated Distillation Column by using *H-xy* and *T-xy* diagrams, Computers and Chemical Engineering, 56, 174–183.

Wakabayashi T., Hasebe S., 2015, Higher Energy Saving with New Heat Integration Arrangement in Heat-Integrated Distillation Column, AIChE Journal, 61, 3479–3488.